Estimating Parallel Transmission Line Fault Using Phasor Measurement Unit based Artificial Neural Network

Surinder Chauhan*, Ratna Dahiya
Department of Electrical Engineering, National Institute of Technology Kurukshetra, Kurukshetra, India.
Email: surinder_6170066@nitkkr.ac.in (Corresponding Author)

Received: May 2021 Revised: August 2021 Accepted: October 2021

ABSTRACT:
In a parallel transmission line, fault line, fault location, and classification have been identified separately. Since fault location takes more calculation time, it is unfit for protection purposes. Thus, this paper presented a new scheme that estimates the faulted line, fault location, and type of fault in a parallel transmission line, with the help of Phasor Measurement Units (PMU) and the Artificial Intelligence Technique. The proposed scheme uses phasors of Positive Sequence Voltage (PSV) and Positive Sequence Current (PSC) to detect the faulted line in a parallel transmission line. Further, the Artificial Neural Network (ANN) models have been designed to estimate the fault distance on a faulted line and classify the fault types. The PSV and PSC obtained from PMUs are selected as inputs because they have a negligible mutual coupling effect on the parallel transmission lines. The IEEE 9 bus system and the IEEE 30 bus system have been considered test cases to validate the proposed scheme. The proposed scheme is also validated by hardware in the loop on an OPAL-RT real-time simulator (OP RTS 5700). The results show that the proposed scheme identifies the fault line, fault distance, and type of fault regardless of its location on a parallel transmission line. Besides this, the proposed scheme has a quick response time, making it suitable for wide-area backup protection applications.

KEYWORDS: Phasor Measurement Unit (PMU), Artificial Neural Network (ANN), Fault analysis.

1. INTRODUCTION

Power system complexity has increased over the last several decades, resulting in the rise of double-circuit and multi-circuit transmission lines. These transmission lines have to work at their maximum power transfer limits to cope with a continuous and adequate quality power supply [1]. Such stressful conditions expose them to faults. It is stated that around 80-90 percent of power grid failures occur on the transmission lines, whereas 10-20 percent of faults are collectively in substation devices and bus bars. [2]. Whenever transmission lines experience a fault, the power supply is interrupted and the utility incurs monetary losses [3]. So, to minimize monetary losses and restore the power supply as quickly as possible, the protection system must identify the fault line and separate it from the healthy portion within a short time [4]. However, most safety relays and breakers mal-operate in fault conditions [5], [6]. It happens due to the hidden failure of the protection system, which causes infeasible or incorrect fault analysis results [5], [6]. In such circumstances, a Wide-Area Monitoring System (WAMS), mainly consisting of Phasor Measurement Units (PMU) and Phasor Data Concentrators (PDC), can be used as backup protection [7]. Moreover, WAMS is more accurate than most traditional backup protection schemes [8]. WAMS uses PMUs to collect data from different places and transfers it to the control centre through the PDCs [9]. Based on the obtained data, different fault location schemes are developed at the control centre. However, the mutual coupling of zero sequence circuits makes assessing faults in parallel transmission lines difficult [10].

2. LITERATURE REVIEW

Over the years, several fault location schemes have been presented. These schemes are mainly classified into conventional schemes [11-14], artificial Intelligence [15-20], signal processing schemes [22-24] and wide-area schemes [25-32]. Conventional schemes are further classified into impedance-based schemes [11-12] and travelling-wave-based schemes [13-14]. The impedance-based schemes use single-end or double-end voltages and bus impedances for fault current and fault location calculations [11], [12]. Such schemes take more computation time, making them unsuitable for the time latency needed for protection purposes. On the other hand, traveling wave-based schemes locate the faults based on the time consumed by the traveling waves from reaching the fault point to one of the terminal buses.

Paper type: Research paper
DOI: https://doi.org/10.52547/mjee.16.1.33
How to cite this paper: S. Chauhan, R. Dahiya,"**Estimating Parallel Transmission Line Fault Using Phasor Measurement Unit based Artificial Neural Network**", Majlesi Journal of Electrical Engineering, Vol. 16, No. 1, pp. 33-47, 2022.

However, such schemes require a higher sampling rate, restricting their usage [13], [14].

Further, different Artificial Intelligence schemes [15]-[20] have been depicted to identify the fault. In [15], the location of fault in faulted transmission line is estimated by an Artificial Neural Network (ANN) based on the Elman recurrent network. In [16], ANN based on the single-end measurement is presented to detect and classify the faults. Later on, the ANN combined with the wavelet transform, such as discrete wavelet transform [17] and S-transform [18], has been used for fault identification. In [19], ANN is used with the filter impulse response, SVM, and SVR to estimate the short-circuit faults in the transmission line. In [20], a convolutional neural network classifier is used to identify the fault distance. All these schemes [15-20] except [17] are limited to identifying faults in single circuit transmission line. In [17], ANN with S-transform has been used to locate fault on parallel transmission line considering single end measurement data. However, single-end measurement data affects the accuracy of fault location under load changes [21]. Beside this, signal processing scheme such as wavelet transform & linear discriminant analysis [22], discrete wavelet transform with harmony search algorithm [23], maximal overlap discrete wavelet transform [24] have been also reported in literature with the assumption of prior information about faulted line.

With the advent of PMUs, various wide-area fault location schemes have been presented [25]-[32]. These schemes utilize the output of the PMUs and attain high accuracy. A fault detection scheme for two bus systems, based on voltage and current phasors, is depicted [25]. However, this work does not include the location and type of faults. Fault location schemes with reduced PMUs are presented in [26] [27], which estimate fault location with prior knowledge of the fault line. They ignore the protection perspective that recognition of a fault line is essential. New fault identification schemes which identify the fault line are considered in [28], [29]. However, these schemes do not identify the exact location of the fault required for maintenance and restoration purposes. A Positive Sequence Voltage (PSV) based iterative fault location scheme, which identifies fault location and fault line, is depicted in [30]. However, due to higher time consumption, this scheme is not suitable for protection proposals. An index-based scheme, with a minimum number of PMUs, is presented in [31], which successfully diagnoses the faulted lines and fault locations. Nevertheless, this scheme is limited to single-circuit transmission lines. Moreover, this scheme does not classify the types of fault. Later on, a fault analysis scheme is presented based on splitting the system into various backup protection zones and current sequence components in [32]. However, the scheme does not apply to parallel transmission lines due to the mutual coupling of zero sequence circuits [10]. A new scheme, based on the current and voltage phasors, has been introduced to estimate the faults in parallel transmission lines [33]. Nevertheless, this scheme is limited to ground faults. Afterwards, a fault recorder with a phase correction method identifies faults in parallel transmission lines [34]. A k-nearest neighbor algorithm is considered, based on single-end measurement, to locate faults in parallel transmission lines in [35]. In [36], the faults are identified in parallel transmission lines when one line is not in used and both ends are grounded. A time-domain based fault location scheme for parallel transmission lines integrated with wind firms is presented in [37]. Moreover, a new fault location scheme based on the Taylor expansion of the distributed line model for the untransposed parallel transmission line is depicted [38]. Besides this, in some schemes compensated transmission lines are considered [39], [40]. In [39], the fault is located on shunt compensated parallel transmission lines, while the fault is located on UPFC compensated transmission lines in [40]. However, detecting fault lines and fault locations was thought to be an independent operation for all these schemes [33-40]. These schemes [33-40] are intended to assess the location of the fault, using pre-knowledge of the transmission line where the fault occurs. Nevertheless, fault line detection has become an important aspect from the protection point of view.

Considering the issues mentioned above, the aim of the proposed scheme is:-

- To detect the faulted line in the parallel transmission line. The faulted line detection has been carried out by exploring the PSV and PSC signals obtained from PMUs.
- To estimate the location of the fault and type of fault on the faulted transmission line. Estimation of fault location and type of faults on faulted line is performed by the ANN models. The ANN models are designed on the basis of the PSV angle, obtained from optimally placed PMUs [41].

The rest of the paper is categorized as follows: Section 3 explains the proposed scheme. The proposed scheme implementation on the IEEE 9 bus system & IEEE 30 bus system is discussed under result & discussion in section 4. Comparative analysis and summary of present work with future scope have been done in section 5 & section 6. Abbreviations used are summarized in section 7.

3. PROPOSED SCHEME

The proposed scheme, which estimates the fault on the parallel transmission line, is explained by considering a sample 5 bus system (Fig. 1).

Fig. 1. Sample 5 bus system.

In a 5-bus system, a parallel transmission line connects bus 3 and bus 4. PMUs are optimally placed in the system on buses 1, 3, and 5. The proposed scheme has identified the fault line, fault distance and type of fault in the below mentioned steps. Further of the proposed scheme flowchart is presented in Fig. 2.

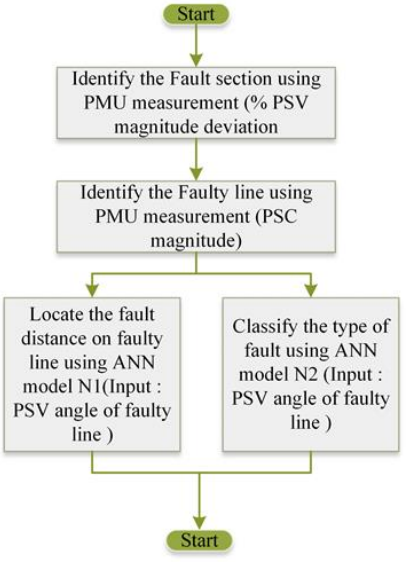

Fig. 2. The proposed Scheme flowchart.

3.1. Identification of the Faulted Line

The determination of the faulted section is the first step in identifying the faulted line. The fault section is determined by the percentage of PSV magnitude deviation measured on PMU buses. The percentage of PSV magnitude deviation is determined by using the pre-fault and during fault PSV magnitude deviations. The percentage of PSV magnitude deviation on the PMU buses remains constant under no-fault conditions. However, in the presence of a fault, the two buses with the highest percentage of PSV deviation entered the fault section. As a result, to locate the 3-phase fault artificially created on a parallel transmission line in a 5 bus system. The PMU buses with a maximum percentage of PSV magnitude deviation, namely PMU bus 3 and PMU bus 5, are selected. To further reduce the faulted section, (1) and (2) are used to calculate the percentage deviation in PSV magnitude at non-PMU bus 4

$$\%V = \frac{V_{prefault} - V_{duringfault}}{V_{prefault}} \times 100 \quad (1)$$

$$V_r = \cosh\gamma l \times V_s - \sinh\gamma l \times I_s \quad (2)$$

It is observed that the percentage PSV magnitude deviation at bus 4 from PMU bus 3 is higher than when it is calculated with PMU bus 5, (3). Therefore, it indicates that the fault is between bus 3 and bus 4.

$$\%V_{43} > \%V_{45} \quad (3)$$

Further, to identify the transmission line with fault, a comparison of the PSC magnitude of each transmission line is done separately, which shows that fault is on transmission lines $3\text{-}4_1$, (4).

$$I_{34_1} > I_{34} \quad (4)$$

3.2. Identification of Fault Location and Classifier using ANN

ANN is one of the most promising machine learning schemes. Its unique feature of determining intricate data patterns has increased its use for different applications. Therefore, in this work ANN architecture is studied. In which**,** two ANN models, i.e., N_1 and N_2, are developed. The N_1 model estimates the fault location at any point in the faulted transmission lines. While N_2 acts as a fault classifier that identifies the type of fault. These ANN models are comprised of the following essential points.

(1) The first step is to select inputs and outputs for ANN. The PSV angle on both ends of the fault line, measured directly or indirectly from PMUs, is considered an input for both ANN models. The distance of the fault from the nearby non-PMU installed bus is regarded as the output of N_1. For the N_2 model, the output is the type of fault represented by the integer value from 1 to 4. Here 1 illustrates a single LG Fault, 2 means LL fault, 3 represents double LG fault, 4 represents a LLL fault.

(2) The next step is selecting the number of layers, neurons per layer, and training algorithm. The ANN architecture with different layers and neurons per layer is tested with various training algorithms. It is found that the back-propagation algorithm is most suitable for the N_1 model and N_2 model

(3) the most crucial point for ANN is training data. It must be such a type that the network is able to discover the essential qualities of the problem. For that reason, the appropriate variety of examples that represent the relative events must be chosen. After the completion of training, they should provide the correct output.

Following the above mentioned essential points. In 5, bus system the PSV angle from both ends of faulted transmission line $3\text{-}4_1$ is given as inputs to the ANN models N_1 and N_2. N_1 determine the distance of fault (in km) from non-PMU bus 4 as shown in Fig. 3.

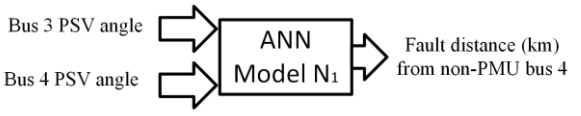

Fig. 3. Fault distance locator.

While N_2 provides the type of fault on the transmission line 3-4_1 i.e. 4, which represents three phase fault (Fig. 4).

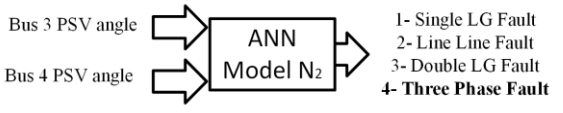

Fig. 4. Fault classifier.

4. RESULT & DISCUSSION

The proposed scheme is simulated in matlab/simulink version 2017b, installed on Intel (R) Core (TM) i5 7200 CPU@ 250 GHz, 2701 Mhz, 4 Core (s) 8 Logical Processor with 4 GB RAM machine. The performance of the proposed scheme is evaluated on two different types of buses: the IEEE 9 bus system and the IEEE 30 bus system. Various fault types are simulated, with differing fault resistance. Further the results have been experimentaly validated by hardware in loop on FPGA based real time simulator (OPRTS 5700). RTS platform comprises a host PC, target simulator, mixed signal oscilloscope (MSO), Bayonet Neill-Concelman (BNC) cables, and a HIL system (see Fig. 29).

4.1. IEEE 9 BUS SYSTEM

In IEEE 9 bus system [42], shown in Fig. 5, Bus 9 to bus 4 is connected through parallel transmission lines, and PMUs are optimally located at buses {4, 6 , 9} using [41]. Different parameters considered for estimation of fault is summarized in Table 1.

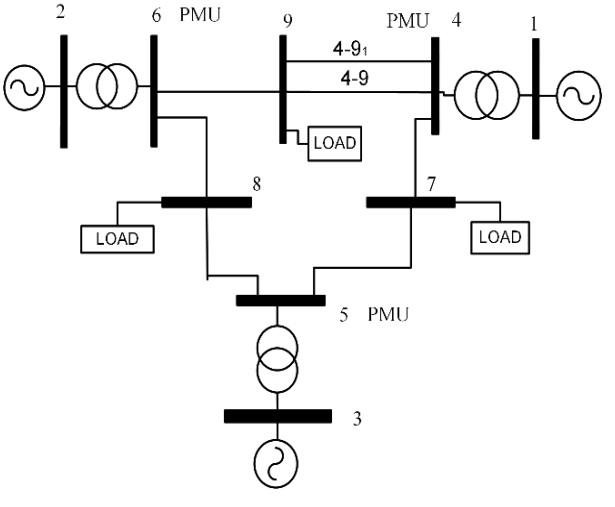

Fig. 5. IEEE 9 bus system.

Table 1. Parameters for fault cases in IEEE 9 bus system.

Type of Faults	SLG, LL, LLG, LLL
Fault Location	50 km, 200 km, 350km
Fault Resistance	0.001Ω, 5Ω, 10Ω, 50Ω

Further, the parameters used to generate a dataset for training and testing the ANN models of fault location and fault classification are summarized in Table 2.

Table 2. Parameters used for data generation.

Parameters	Training Dataset	Testing Dataset
Fault Types	SLG, LL, LLG, LLL	SLG, LL, LLG, LLL
Fault Resistance	0.001Ω, 5 Ω 10 Ω, 50 Ω	0.001Ω, 5 Ω 10 Ω, 50 Ω
Fault Location (km)	10 20 30 40 50 70…….390	15 25 35 45 55 65…….395

The proposed ANN fault locator (N1) & ANN fault classifier (N2) are trained by a back propagation algorithm, and generalization is implemented using early stopping. Early stopping divides the data into 70 % learning data, 15 % testing data and 15 % validation data. Further, routine 'postreg' is determined by the performance of trained networks. It conducts a regression analysis between the network response and the associated targets. Fig. 6 and Fig. 7 show the graphical output produced by postreg for the N1 and N2 models, respectively. The graphical output shows the regression analysis of training, testing, validation, and combined data. In which, R represents the correlation coefficient between the outputs and targets. The correlation coefficients indicate how well targets account for output variance. If this value is equal to 1, then the targets and outputs are perfectly correlated. Although the correlation coefficient (R) value in each model is near 1, indicating that output tracks the target reasonably well, Moreover, in Fig. 6 and Fig. 7, the network outputs are shown as open circles against the targets, and a best linear fit is denoted by dashed line. An ideal match i.e. output=targets is represented through solid line. However, because the fit is so good, it is not easy to discern between the best linear fit line and the perfect fit line in both cases.

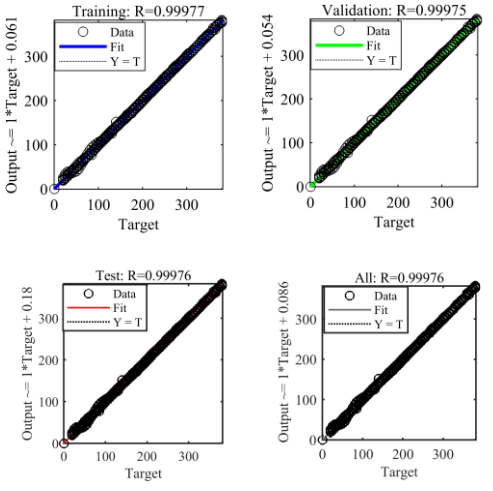

Fig. 6. Regression performance analysis of ANN fault Locator (N1).

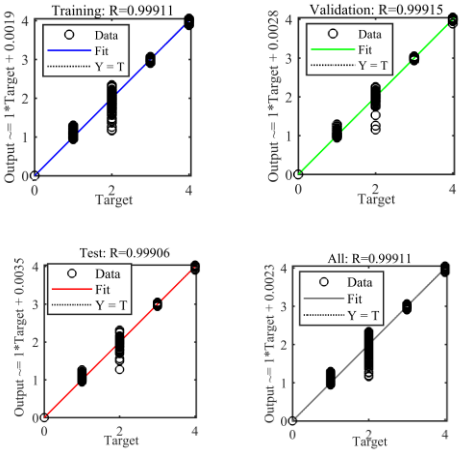

Fig. 7. Regression performance analysis of ANN fault Classifier (N2).

Further, the validation evaluations for the N1 and N2 models is indicated in Fig. 8 and Fig. 9. It displays the mean square error between target and network outputs. Validation is used to keep a check on the data from being overfitted. Typically, the validation set error starts to climb when the network begins to overfit the data. The training is terminated if the validation error persists after a certain number of iterations. The best validation performance in the N1 model is 0.5268 at 580 epochs (Fig. 8), while in the N2 model, it is 0.0019538 at 125 epochs (Fig. 9).

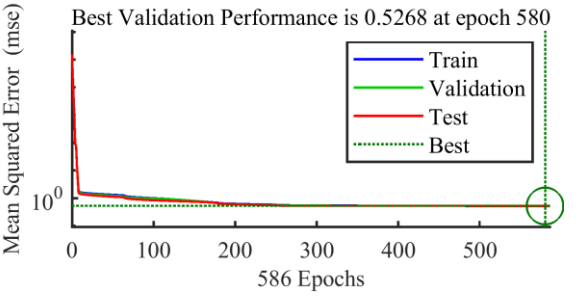

Fig. 8. Validation evaluation of N1 model.

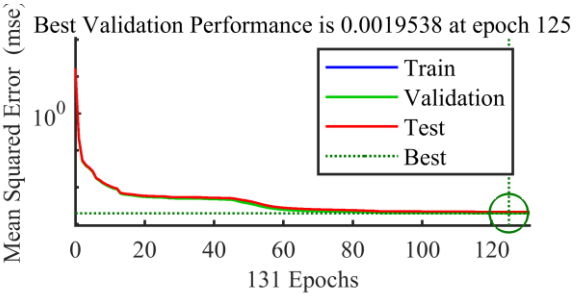

Fig. 9. Validation evaluation of N2 model.

Further the implementation of the proposed scheme are discussed as follows

4.1.1. LLG fault near to bus 9

A double line to a ground fault having a 50 Ω resistance is created at 0.5 seconds on parallel transmission lines (connecting between buses 4 to 9) at 50 km from non-PMU bus 9. According to the proposed scheme, the percentage PSV magnitude deviation on all PMU buses is measured (Fig 10).

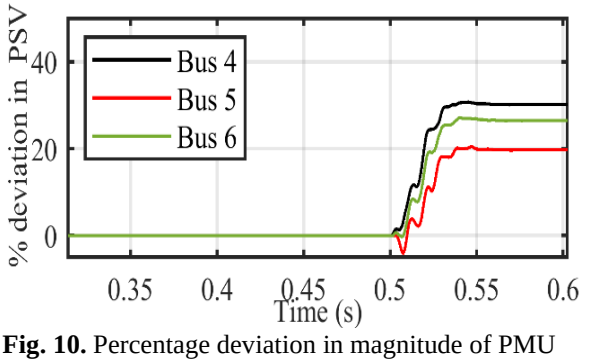

Fig. 10. Percentage deviation in magnitude of PMU buses.

The two PMU buses, i.e., bus 4 & bus 6, having maximum PSV deviation, identify the faulted section. After that, the PSV deviation is computed at non-PMU bus 9 (Fig. 11), which confined the faulted section from bus 4 to bus 9 (Fig. 11).

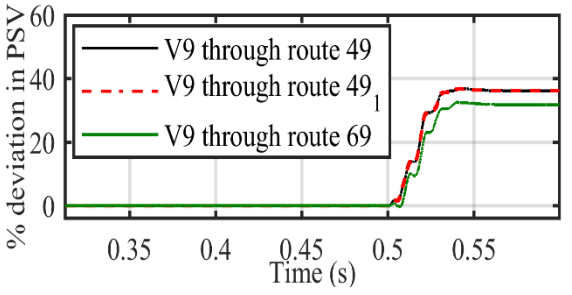

Fig. 11. Percentage deviation in PSV magnitude at bus 9.

Further, to identify the faulted transmission line in the faulted section (bus 4 to bus 9) having a parallel transmission line, the PSC magnitude of each transmission line is computed. The transmission line (4-9_1) has a higher PSC magnitude than other transmission lines 4-9 (Fig. 12). Therefore transmission line 4-9_1 is detected as the faulted line within 39.06 msec.

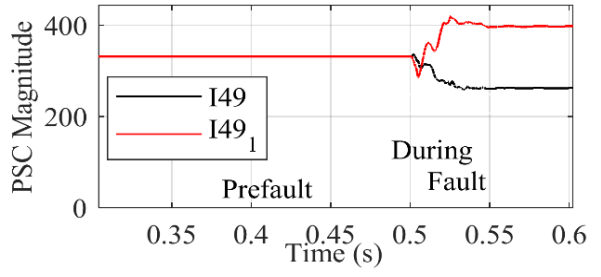

Fig. 12. PSC magnitude of parallel transmission lines.

After identifying the faulted line, the PSV angle of both end buses of the faulted line is fed to the neural networks N_1 and N_2. N_2 accurately classified the type of fault and N_1 locate the fault on transmission lines 4-9_1 at sample number 1365 (Fig. 13) within 33.6 msec as stated.

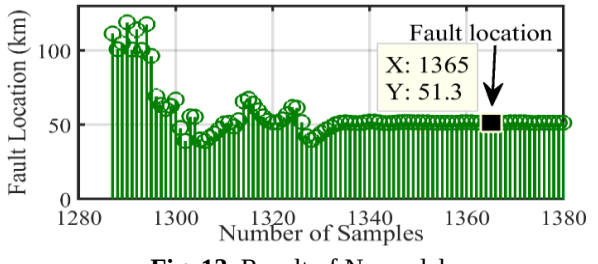

Fig. 13. Result of N_1 model.

Fault location time = [(sample number at which fault locate)-(sample number at which fault detected) * sample time]

Fault location time = [(1365-1285)*0.00042] = 33.6 msec

However, considering the WAMS communication delay of 200 msec in either direction [43], The proposed scheme estimates the fault line and location of fault within 472.6 msec

The percentage fault location error is given as [14]

$$\%\ error = \frac{|\ actual\ \ fault\ location - estimated\ \ fault\ location\ |}{length\ of\ \ line} \quad (5)$$

$$\%\ error = \frac{|\ 50 - 51.3\ |}{400} \times 100 = 0.33 \quad (6)$$

4.1.2 Three Phase fault at a distance of 200 km from bus 9

The proposed scheme performance is tested on the middle of transmission line by creating the LLL fault with 10 Ω on the midpoint of the parallel transmission. According to the proposed scheme, the percentage of PSV magnitude deviation on all PMU buses is measured (Fig 14).

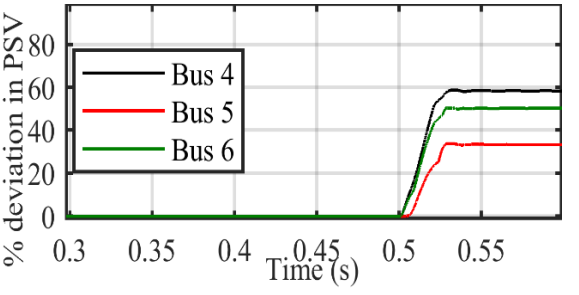

Fig. 14. Percentage deviation in magnitude of PMU buses.

The two PMU buses, having maximum percentage magnitude deviation, namely bus 4 and bus 6 made the faulted section. The faulted section is further confined to 4-9 by computing the PSV magnitude deviation (percentage) at non-PMU bus 9, shown in Fig. 15.

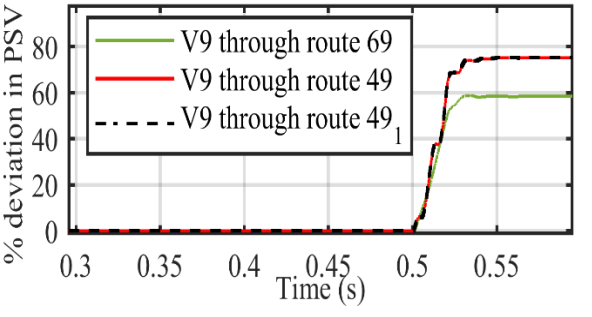

Fig. 15. PSV calculated at bus 9.

Furthermore, PSC magnitude of each transmission line is computed to detect the faulted transmission line in the faulted section (4-9) that has a parallel transmission line. The transmission line with the maximum PSC magnitude is identified as the faulted line as shown in Fig. 16.

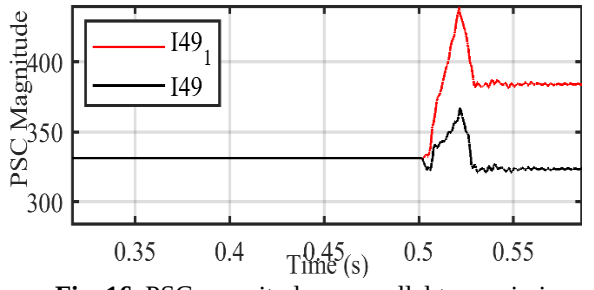

Fig. 16. PSC magnitude on parallel transmission line.

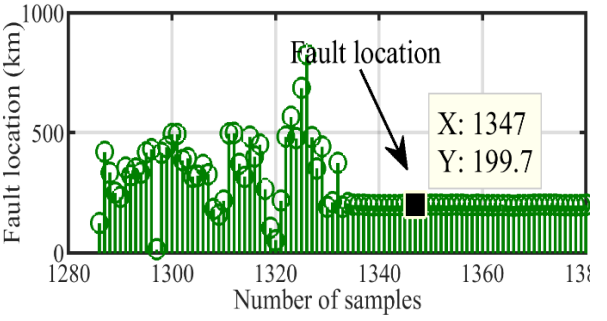

Fig. 17. Result of N_1 model.

Table 3. Estimation of fault at bus 9 in IEEE 9 bus system.

Fault Type	Fault resistance (Ω)	Estimated Fault line	Estimated Fault location for 50 km		Estimated Fault location for 200 km		Estimated Fault location for 350 km		Estimated Fault Type
			N_1 Output	% error	N_1 Output	% error time	N_1 Output	% error time	N_2 output
SLG	0.001	4-9$_1$	49.73	0.07	199.56	0.11	349.48	0.13	1
LL		4-9	50.56	0.14	200.58	0.15	349.28	0.18	2
LLG		4-9	50.48	0.12	200.30	0.08	349.40	0.15	3
LLL		4-9$_1$	49.40	0.15	199.31	0.17	349.24	0.19	4
SLG	5	4-9$_1$	49.57	0.10	199.64	0.12	350.44	0.14	1
LL		4-9	50.74	0.18	199.24	0.19	349.20	0.21	2
LLG		4-9$_1$	50.59	0.15	199.44	0.14	350.52	0.13	3
LLL		4-9	50.51	0.13	199.56	0.11	349.52	0.12	4
SLG	10	4-9	50.42	0.12	199.48	0.13	349.48	0.15	1
LL		4-9$_1$	51.23	0.31	198.72	0.32	348.80	0.30	2
LLG		4-9	50.86	0.21	199.20	0.20	349.24	0.19	3
LLL		4-9$_1$	50.81	0.20	199.70	0.21	349.08	0.23	4
SLG	50	4-9	51.11	0.28	199.08	0.23	348.96	0.26	1
LL		4-9$_1$	51.74	0.43	201.76	0.44	351.72	0.43	2
LLG		4-9	51.30	0.33	198.80	0.30	348.76	0.31	3
LLL		4-9$_1$	51.05	0.27	201.24	0.31	348.88	0.28	4

1=Single LG fault, 2=LL fault, 3 = LLG fault, 4 = LLL fault

After identifying the faulted line, the PSV angle of both end buses of the faulted line is fed to the neural networks N_1 and N_2. N_1 estimated the fault location on transmission lines 4-9 at sample no 1347 within 26.04 msec after detection of fault at 1285 sample, as indicated in Fig. 17. The percentage error obtained in the fault location is 0.21.

4.1.3. L-L fault at a distance of 350 km from bus 9

The performance of proposed scheme performance for far-end faults is evaluated by creating a fault within 0.5 sec on parallel transmission lines 4-9. The fault occurred 350 km away from the bus 9 and had a fault resistance of 5 ohms. The proposed scheme measures the percentage of PSV magnitude deviation on all PMU buses. (Fig. 18).

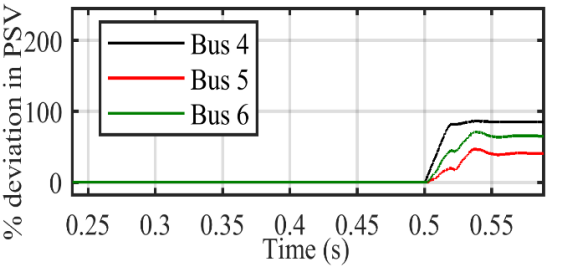

Fig. 18. PSV at PMU buses.

The fault section is identified by the two PMU buses with the maximum PSV deviation, namely bus 4 and bus 6. The PSV deviation is then computed on non-PMU bus 9 (Fig. 19), which limits the faulted section from bus 4 to bus 9. Furthermore, the PSC magnitude of each transmission line is computed in order to identify the

faulted transmission line in the faulted section (bus 4 to bus 9) that has a parallel transmission line. The transmission line with the greatest PSC magnitude rise is considered as the fault line. Following that, the PSV angle at both ends of the faulted transmission line is fed into the N1 and N2 models, which classify and locate the fault. Within 28.56 msec, N1 identified the fault on transmission lines 4-9 at sample number 1353, as shown in Fig. 20.

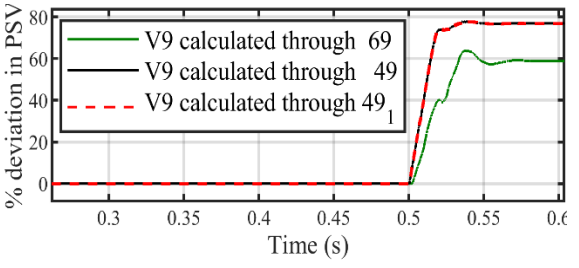

Fig. 19. PSV at bus 9.

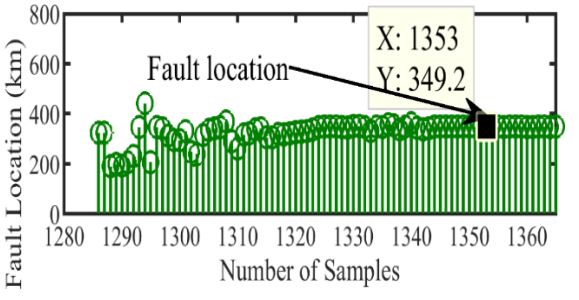

Fig. 20. Result of N_1.

Table 3 summarizes the other types of faults with varying fault resistance. It is worth noting that, regardless of the fault location, the percentage of errors at each fault location almost falls within the same range (Fig. 21).

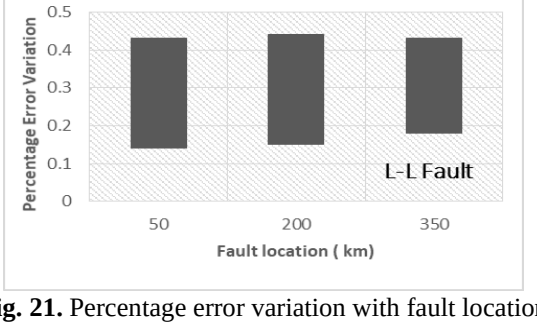

Fig. 21. Percentage error variation with fault location LL fault.)

4.2. IEEE 30 BUS SYSTEM

The proposed scheme performance is further tested on the IEEE 30 bus system [44] in which transmission lines connected from bus 1 to bus 2 are considered a parallel transmission line, (Fig. 22). The PMUs are optimally placed at bus {2, 3 5, 7, 9, 11, 13, 15, 17, 19, 21, 23, 25, 27, 29}. Different parameters considered for estimation of fault is summarized in Table 4

Table 4. Parameters used for fault estimation.

Type of Faults	SLG, LL, LLG, LLL
Fault Location	50 km, 200 km, 350km
Fault Resistance	0.001Ω, 5Ω, 10Ω, 50Ω

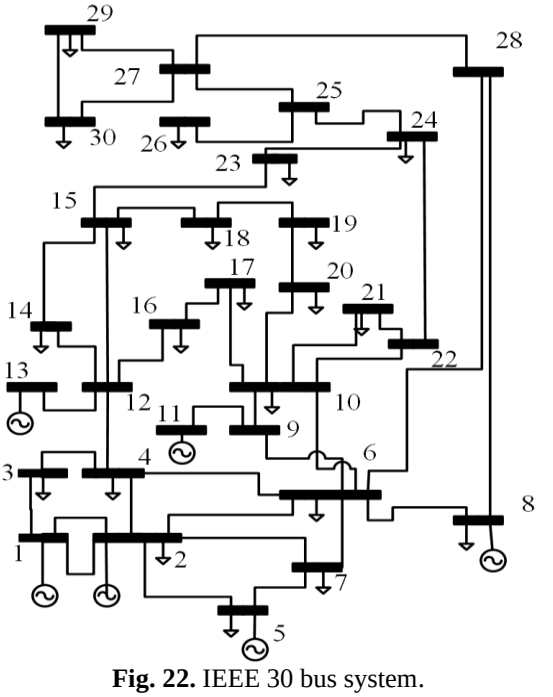

Fig. 22. IEEE 30 bus system.

Further, the parameters used to generate a dataset for training and testing the ANN is summarized in Table 5.

Table 5. Parameters used for data generation.

Parameters	Training Dataset	Testing Dataset
Fault Types	SLG, LL, LLG, LLL	SLG, LL, LLG, LLL
Fault Resistance	0.001Ω, 5 Ω 10 Ω, 50 Ω	0.001Ω, 5 Ω 10 Ω, 50 Ω
Fault Location (km)	10 20 30 40 50 70…….140	15 25 35 45 55 65…….135

It is found that the proposed ANN fault locator (N1) is trained by back propagation algorithm with 75 % learning data, 15 % testing data and 15 % validation data as shown in Fig. 23.

Table 6. Estimation of fault in IEEE 30 bus system.

Fault Type	Fault resistance (Ω)	Estimated Fault location for 20 km		Estimated Fault location for 70 km		Estimated Fault location for 120 km		Estimated Fault Type
		N_1 Output	Percentage Error	N_1 Output	Percentage Error	N_1 Output	Percentage Error	N_2 output
SLG	0.001	19.93	0.05	69.91	0.06	119.94	0.04	1
LL		19.86	0.10	69.89	0.08	119.81	0.13	2
LLG		20.22	0.16	70.23	0.16	200.21	0.15	3
LLL		19.73	0.19	69.65	0.25	119.71	0.21	4
SLG	5	19.87	0.09	69.89	0.08	119.85	0.11	1
LL		19.73	0.19	69.71	0.21	119.79	0.15	2
LLG		19.81	0.14	69.86	0.10	119.84	0.11	3
LLL		19.74	0.19	69.72	0.20	119.70	0.21	4
SLG	10	20.21	0.15	70.26	0.19	200.28	0.20	1
LL		19.67	0.24	69.63	0.26	119.60	0.29	2
LLG		20.31	0.22	70.36	0.26	200.39	0.28	3
LLL		20.32	0.23	70.35	0.25	200.34	0.24	4
SLG	50	19.58	0.30	70.48	0.34	119.55	0.39	1
LL		19.41	0.42	69.43	0.41	119.44	0.40	2
LLG		19.56	0.31	69.54	0.33	119.59	0.29	3
LLL		20.44	0.31	70.47	0.34	200.49	0.35	4

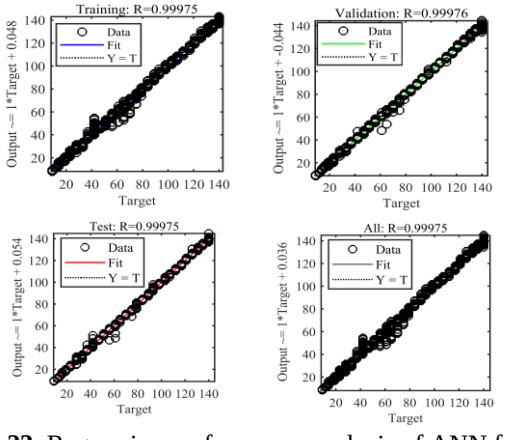

Fig. 23. Regression performance analysis of ANN fault Locator (N1).

Fig. 24 exhibits the best validation performance accompanied by validation assessment.

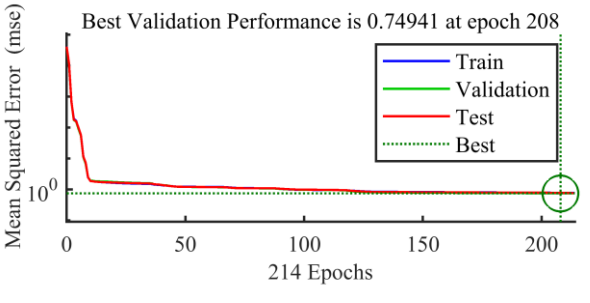

Fig. 24. Validation evaluation of ANN fault Locator (N1).

Further the implementation of the proposed scheme on IEEE 30 bus system under different fault types are discussed as follows.

4.2.1. Single LG fault near bus 1

A fault having an unknown type and location with a fault resistance of 50 ohm is created at 0.5 sec on the IEEE 30 bus system. To estimate the fault, the proposed scheme determines the percentage of PSV magnitude deviation on different PMU buses, Fig 25 (a).

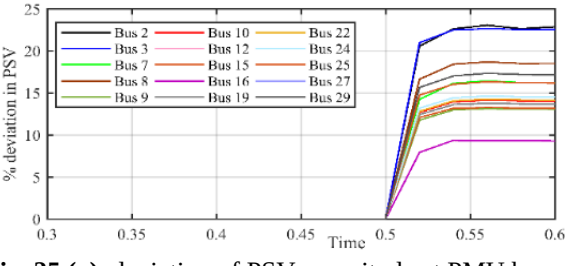

Fig. 25 (a). deviation of PSV magnitude at PMU buses.

From Fig. 25 (a), it can be interpreted that PMU bus 2 and PMU bus 3 have a maximum PSV deviation. Therefore, according to the proposed scheme, the fault lies in the paths between bus 2 & bus 3. After that, the PSV percentage deviation is calculated on non-PMU buses, which lie in the path connecting bus 2 to bus 3. It is found that the PSV deviation on the non-PMU bus 1 calculated from the PMU bus 2 and PMU bus 3 is mismatched, Fig. 25 (b).

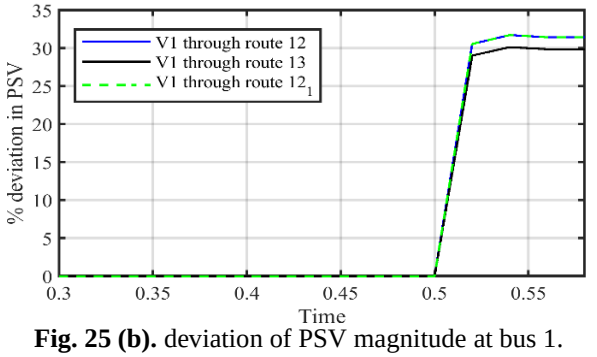

Fig. 25 (b). deviation of PSV magnitude at bus 1.

Fig. 25 (b) shows that the PSV deviation on non-PMU bus 1 calculated from PMU bus 2 is higher than on PMU bus 3. Therefore, the fault lies in the transmission lines connecting bus 1 to bus 2. However, parallel transmission lines exist between bus 1 and bus 2. So, to identify the exact fault line, the change in the magnitude of the PSC of both transmission lines is calculated. The rise in current magnitude is higher in the faulted line than in the other lines, as shown in Fig. 25 (c). From Fig. 25 (c), it can be found that transmission line 1-2$_1$ is a faulted line

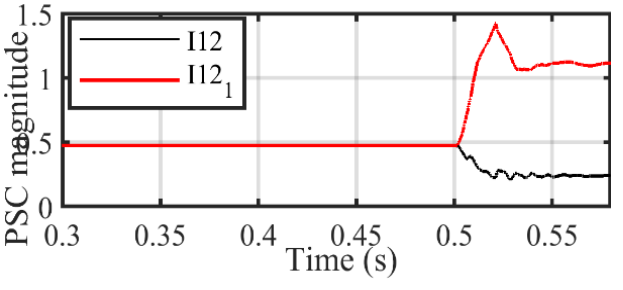

Fig. 25 (c). PSC when L-G fault occurs on transmission line 1-2$_1$.

Further, to check the type and distance of a fault on the faulted line, the PSC angle of both sides of the faulted transmission line is given as input to the ANN model N_1 and ANN model N_2. N_1 has located the fault on transmission lines 1-2$_1$ at sample number 1337, as shown in Fig. 25 (d). The time required to locate the fault is 21.84.5 msec ((1337-1285) * 0.00042), with a 0.32 % error in fault location.

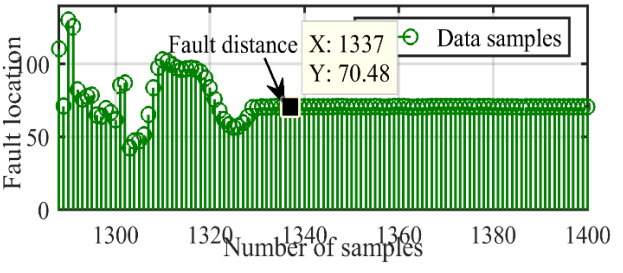

Fig. 25 (d). Result of N_1 under L-G fault.

The other types of faults with different fault resistance are summarized in Table 6. It should be noted that the proposed scheme is irrespective of the fault locations. The percentage of error at each fault location almost lies in the same range (Fig. 26)

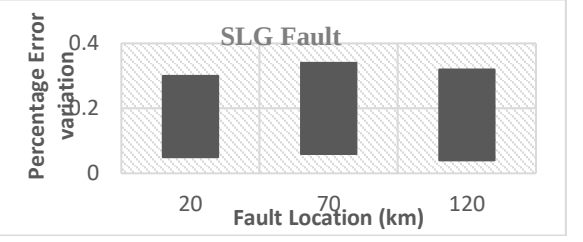

Fig. 26. Percentage error variation with fault location.

4.3. Proposed Scheme Under Stressed Power Sytem Conditions

A good fault identification scheme should not operate under stressed power system conditions such as load change, generator outage etc., under no-fault. Therefore, an appropriate threshold value is required that distinguishes the fault from other power system stressed conditions. In the suggested scheme, the threshold value is selected at 5 % PSV magnitude deviation based on the various fault simulation instances. The usefulness of the selected threshold value is demonstrated by simulating the two scenarios below using the IEEE 30 bus system.

4.3.1. Load Change

In this scenario, the load on bus 2 is increased at 0.5 sec to P=43.4 MW & Q=25.2 MW. The percentage PSV deviation is calculated at each PMU bus (Fig. 27).

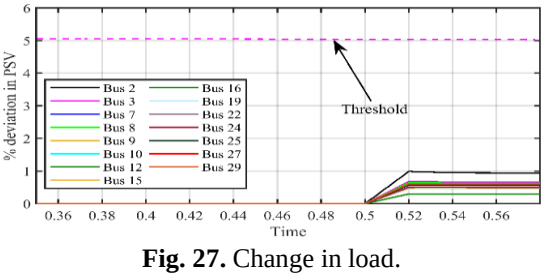

Fig. 27. Change in load.

No PMU bus violates the threshold limits. Hence the proposed scheme has not considered this scenario as a fault in the test system.

4.3.2. Generator Outage

A scenario is simulated in which the generator goes down at bus 1 after 0.5 sec. Each PMU bus calculated the percentage of PSV magnitude deviation (Fig. 28). The threshold limits are not exceeded by any PMU bus. As a result, the proposed scheme has not treated this scenario as a fault in the test system

Table 7. Comparative analysis.

Papers	Fault line detection	Fault type detection	Percentage fault location error		
			min	max	Average
Ref [33]	✓	__	0.07	0.49	0.28
Ref [34]	__	__	0.02	0.43	0.23
Ref [35]	__	__	0.00	1.3	0.65
Ref [45]	__	__	0.11	0.45	0.28
Ref [46]	__	__	0.06	0.44	0.25
Proposed Scheme	✓	✓	0.04	0.40	0.22

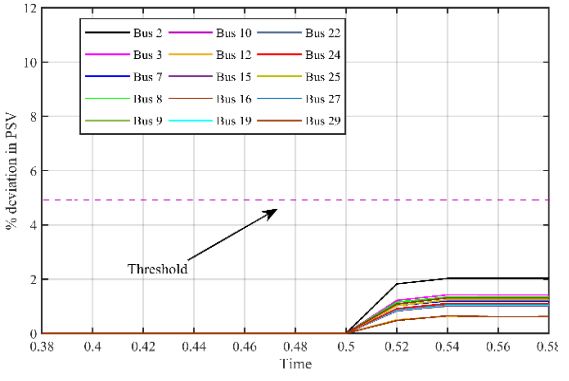

Fig. 28. Generator outage at bus 1.

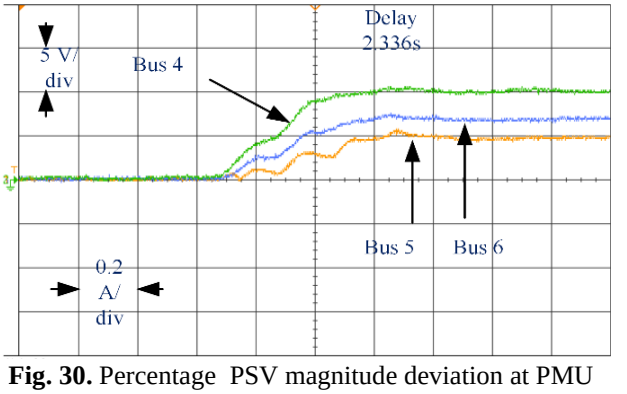

Fig. 30. Percentage PSV magnitude deviation at PMU buses.

4.4. REAL-TIME SIMULATION

The Simulink results are validated by deploying the IEEE 9 bus system with simulated PMUs in the RTS platform (OP5700 RTS), Fig. 29. RTS platform comprises a host PC, one digital storage oscilloscope (DSO), Bayonet Neill-Concelman (BNC) cables, and a HIL system.

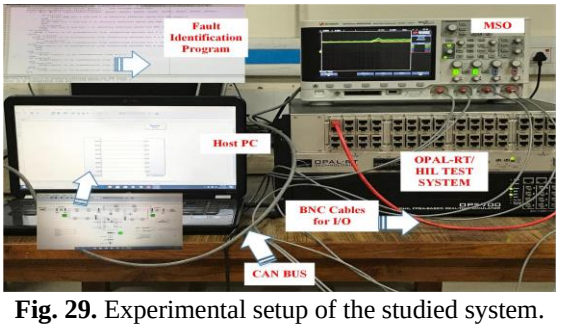

Fig. 29. Experimental setup of the studied system.

In the case of LLG fault on a parallel transmission line (bus 4 -bus 9), the waveform of percentage magnitude of PSV deviation at PMU buses on OPAL-RT simulator is shown in Fig. 30. It shows that bus 4 & bus 6, having maximum PSV deviation, made the faulted section.

Likewise, the percentage PSV magnitude deviation is obtained at non-PMU bus 9, shown in Fig. 31, which confined the fault section from bus 4 to bus 9.

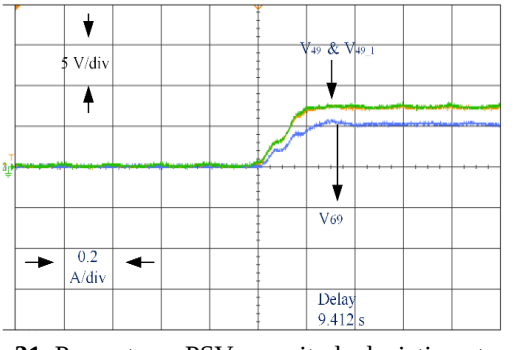

Fig. 31. Percentage PSV magnitude deviation at non-PMU bus 9.

Further, the fault section 4-9 have a parallel transmission lines. Therefore if fault is on transmission line 4-9_1 than there is rise in PSC magnitude of 4-9_1 line (Fig. 32) .However if fault is on transmission line 4-9, then there is rise in PSC magnitude of 4-9 line (Fig. 33).

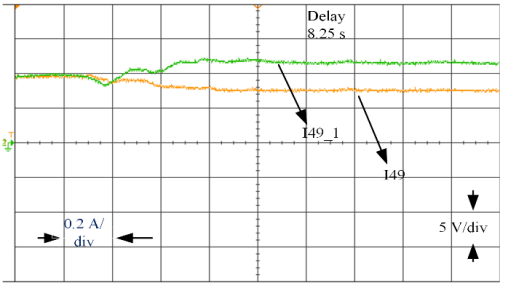

Fig. 32. Rise in PSC magnitude at transmission line 4-9_1.

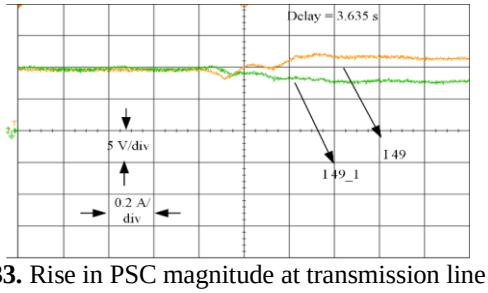

Fig. 33. Rise in PSC magnitude at transmission line 4-9.

5. COMPARISON WITH OTHER WORKS

In this section, the effectiveness of the proposed scheme has been determined by comparing it with other schemes available in the literature. The existing schemes [33], [34], [35], [45] and [46] are simulated in MATLAB/Simulink for all types of fault cases in the IEEE 9 bus system. The results obtained are compared with the proposed scheme. The findings are summarized in Table 7. The table shows that the existing schemes only detect the location of the fault, except [33], which also detects the fault line. However, the [33] scheme is only applicable to LG faults.

On the other hand, the proposed scheme not only identifies the faulted line and type of fault but also estimates the location of the fault. The proposed scheme estimates the fault location with an average error of 0.22 per cent, which is the minimum as compared to other existing schemes. Moreover, Table 8 shows the comparison of fault location time of the proposed scheme with other PMU based existing schemes [33], [49], [50]. It shows that the proposed scheme has a reasonably quick response time.

Table 8. Average fault location time.

Papers	Average Fault Location time (msec)
[33]	40.75
[35]	60
[48]	71
[49]	< 52 sec
Proposed Scheme	30.21

Besides this, the proposed scheme is compared with the existing scheme [33] in Table 9, considering different parameters. Further, the comparison of fault location error at different fault locations on IEEE 9 bus system considering SLG fault for existing scheme [33] and proposed scheme is given in Fig. 34. The main advantage of the proposed scheme over the existing scheme [33] is its fault location accuracy and applicability for all types of faults.

Table 9. Comparison with Ref [33] for SLG fault.

Sr. No	Ref [33]	Proposed Scheme
Faulted line	6-9	6-9
Estimated Fault type	__	S-LG
Percentage fault location error	0.49	0.15
Average Fault location time (msec)	40.75	30.21
Delay time (msec)	400	400
Stressed power system condition	Not Reported	Works under stressed conditions

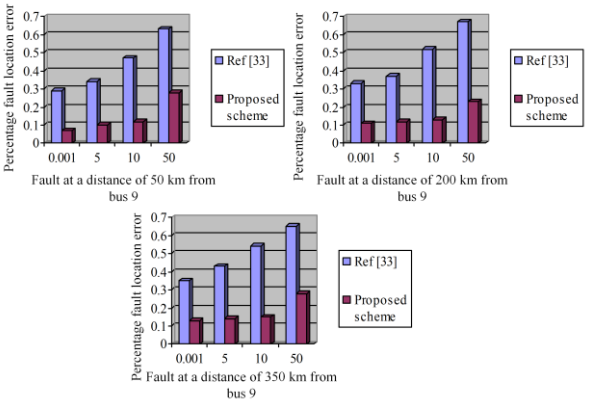

Fig. 34. Comparison of the proposed scheme with Ref [33] for SLG fault.

6. CONCLUSION

A simple yet efficient fault estimation scheme, which estimated the fault in a parallel transmission line, was proposed in this paper. The proposed scheme had used a phasor of PSV and PSC, obtained from PMUs, in ANN to identify the faulted line, fault distance (from the non-PMU bus), and type of faults in a parallel transmission line. It does not require any phase correction algorithm and also yields high accuracy even under stressed power system conditions such as load change, generator outage. Added advantage of the proposed scheme is that it can detect the presence of a fault within 470 milliseconds (including communication delay), making

it appropriate for wide-area backup protection applications.

Extensive simulations involving various faults at different distances and varying fault resistance on the IEEE 9 bus system and the IEEE 30 bus system validated the suggested scheme. The results show that the suggested scheme accurately identified, classified, and located the fault regardless of its location on the parallel transmission line. The proposed scheme performance may be tested under high fault resistance for unbalanced active distribution networks as a future perspective.

7. NOMENCLATURE

ANN : Artificial Neural Network
PMU : Phasor Measurement Unit
PDC : Phasor Data Concentrator
PSC : Positive Sequence Current
PSV : Positive Sequence Voltage
WAMS : Wide Area Monitoring System
N_1 : ANN fault locator
N_2 : ANN fault classifier
% V : Percentage deviation in PSV
$V_{prefault}$: Positive Sequence Voltage before fault
$V_{duringfault}$: Positive Sequence Voltage during fault
$\%V_{43}$: Percentage deviation in PSV at bus 4 through PMU bus installed at bus 3
$\%V_{45}$: Percentage deviation in PSV at bus 4 through PMU bus installed at bus 5
I_{34} : PSC magnitude at transmission line 3-4
I_{34_1} : PSC magnitude at transmission line 3'-4'

8. APPENDIX

A vast number of simulations have been used to determine the PSV deviation threshold value. In each simulation, the PSV magnitude is computed at i_{th} bus through different routes (buses connected to the i_{th} bus) under no-fault conditions. It is to be supposed that the PSV calculated at i_{th} bus through different routes remains the same under no-fault conditions. However, PSV obtained from different routes may not be equal due to the flaws in the measuring equipment [50], which leads to a false result. Therefore, to keep things under control, a threshold value of PSV deviation is selected which is computed as

$$\%\,PSV = \max\left(\frac{\left|PSV_{\max}\right| - \left|PSV_i\right|}{\left|PSV_i\right|} \times 100\right) \qquad (7)$$

Where,

i = 1,…..,z

z is the total number of buses connected to the i_{th} bus through which PSV_i is calculated and $PSV_{\max}$ is the maximum value of PSV_i.

9. ACKNOWLEDGMENT

Gratitude to the Ministry of Human Resource Development, Government of India, for giving financial aid for this study.

REFERENCES

[1] P. Chen, Q. Xu, Y. Ge, G. Song, and J. Suonan, "**Parallel Transmission Lines Fault Location Algorithm Based on Differential Component Net**," *IEEE Trans. Power Deliv*., Vol. 20, No. 4, pp. 2396–2406, 2005.

[2] X. Liang, S. A. Wallace, and D. Nguyen, "**Rule-Based Data-Driven Analytics for Wide-Area Fault Detection Using Synchrophasor Data,**" *IEEE Transactions on Industry Applications*, Vol. 53, No. 3, pp. 1789-1798, 2017.

[3] N. Kang and Y. Liao, "**Double-Circuit transmission-line fault location utilizing synchronized current phasors***," IEEE Trans. Power Deliv.*, Vol. 28, No. 2, pp. 1040–1047, 2013.

[4] M. M. Eissa, M. E. Masoud, and M. M. M. Elanwar, "**A novel back up wide area protection technique for power transmission grids using phasor measurement unit**," *IEEE Trans. Power Deliv*., Vol. 25, No. 1, pp. 270–278, 2010..

[5] W.-H. Chen, S.-H. Tsai and H.-I. Lin, "**Fault Section Estimation for Power Networks Using Logic Cause-Effect Models**," *IEEE Transactions on Power Delivery*, Vol. 26, No. 2, pp. 963-971, 2011.

[6] W. A. dos Santos Fonseca, U. H. Bezerra, M. V. A. Nunes, F. G. N. Barros, and J. A. P. Moutinho, "**Simultaneous Fault Section Estimation and Protective Device Failure Detection Using Percentage Values of the Protective Devices Alarms**," *IEEE Transactions on Power Systems*, vol. 28, No. 1, pp. 170-180, 2013.

[7] A. G. Phadke, P. Wall, L. Ding, and V. Terzija, "**Improving the performance of power system protection using wide area monitoring systems***," J. Mod. Power Syst. Clean Energy*, Vol. 4, No. 3, pp. 319–331, 2016.

[8] Heng-xu Ha, Bao-hui Zhang and Zhi-lai Lv, "**A novel principle of single-ended fault location technique for EHV transmission lines,**" *IEEE Transactions on Power Delivery*, Vol. 18, No. 4, pp. 1147-1151, 2003.

[9] X. Zhu, M. H. F. Wen, V. O. K. Li, and K. C. Leung, "**Optimal PMU-Communication Link Placement for Smart Grid Wide-Area Measurement Systems**," *IEEE Trans. Smart Grid*, Vol. 10, No. 4, pp. 4446–4456, 2019.

[10] M.M. Saha, Network Configurations and Models. In: *Fault Location on Power Networks*. Power Systems, London, Springer, 2010.

[11] Y. Liao, "**Fault Location Utilizing Unsynchronized Voltage Measurements During Fault**,*" Electric Power Components and Systems*, Vol. 34, No. 12, pp. 1283-1293, 2007.

[12] A. Gopalakrishnan, M. Kezunovic, S. M. McKenna, and D. M. Hamai, "**Fault location using the distributed parameter transmission line model**," *IEEE Transactions on Power Delivery*, Vol. 15, No. 4, pp. 1169–1174, 2000.

[13] J. Ding, X. Wang, Y. Zheng, and L. Li, "**Distributed Traveling-Wave-Based Fault-Location Algorithm Embedded in Multiterminal Transmission Lines**," *IEEE Transactions on Power Delivery*, Vol. 33, No. 6, pp. 3045-3054, 2018.

[14] O. D. Naidu and A. K. Pradhan, "**A Traveling Wave-Based Fault Location Method Using Unsynchronized Current Measurements**," *IEEE Transactions on Power Delivery*, Vol. 34, No. 2, pp. 505-513, 2019.

[15] S. Ekici, S. Yildirim, M. Poyraz, "**A transmission line fault locator based on Elman recurrent networks**," *Applied Soft Computing*, Vol 9, No. 1, pp. 341-347, 2009.

[16] M. Jamil, S. K. Sharma, and R. Singh, "**Fault detection and classification in electrical power transmission system using artificial neural network**," *Springerplus*, Vol. 4, No. 1, p. 334, Dec. 2015.

[17] A. Yadav and A. Swetapadma, "**A single ended directional fault section identifier and fault locator for double circuit transmission lines using combined wavelet and ANN approach**," *Int. J. Electr. Power Energy Syst.*, Vol. 69, pp. 27–33, Jul. 2015.

[18] N. Roy and K. Bhattacharya, "**Detection, classification, and estimation of fault location on an overhead transmission line using s-transform and neural network**," *Electr. Power Components Syst.*, Vol. 43, No. 4, pp. 461–472, 2015.

[19] H. Fathabadi, "**Novel filter based ANN approach for short-circuit faults detection, classification and location in power transmission lines**," *Int. J. Electr. Power Energy Syst.*, Vol. 74, pp. 374–383, 2016.

[20] W. Li, D. Deka, M. Chertkov, and M. Wang, "**Real-Time Faulted Line Localization and PMU Placement in Power Systems Through Convolutional Neural Networks**," *IEEE Trans. Power Syst.*, Vol. 34, No. 6, pp. 4640–4651, Nov. 2019.

[21] T. Hinge and S. Dambhare, "**Synchronised/unsynchronised measurements based novel fault location algorithm for transmission line**," *IET Gener. Transm. Distrib.*, Vol. 12, No. 7, pp. 1493–1500, Apr. 2018.

[22] A. Yadav and A. Swetapadma, "**A novel transmission line relaying scheme for fault detection and classification using wavelet transform and linear discriminant analysis**," *Ain Shams Eng. J.*, Vol. 6, No. 1, pp. 199–209, Mar. 2015.

[23] T. S. Abdelgayed, W. G. Morsi, and T. S. Sidhu, "**Fault detection and classification based on co-training of semisupervised machine learning**," *IEEE Trans. Ind. Electron.*, Vol. 65, No. 2, pp. 1595–1605, 2017.

[24] V. Ashok and A. Yadav, "**A real-time fault detection and classification algorithm for transmission line faults based on MODWT during power swing**," *Int. Trans. Electr. Energy Syst.*, Vol. 30, No. 1, pp. 1–27, 2020.

[25] A.G. Phadke, M. Ibrahim, and T. Hlibka, "**Fundamental basis for distance relaying with symmetrical components**," *IEEE Transactions on Power Apparatus and System*, Vol. 96, No. 2, pp. 635–646, 1977.

[26] A. Salehi-Dobakhshari and A. M. Ranjbar, "**Robust fault location of transmission lines by synchronised and unsynchronised wide-area current measurements,**" *IET Generation, Transmission & Distribution*, Vol. 8, No. 9, pp. 1561-1571, 2014.

[27] A.S. Dobakhshari and A. M. Ranjbar, "**A Novel Method for Fault Location of Transmission Lines by Wide-Area Voltage Measurements Considering Measurement Errors**," *IEEE Transactions on Smart Grid*, Vol. 6, No. 2, pp. 874-884, 2015.

[28] M. M. Eissa, M. E. Masoud, and M. M. M. Elanwar, "**A Novel Back Up Wide Area Protection Technique for Power Transmission Grids Using Phasor Measurement Unit**," *IEEE Transactions on Power Delivery*, Vol. 25, No. 1, pp. 270-278, 2010.

[29] B. K. Saha Roy, R. Sharma, A. K. Pradhan, and A. K. Sinha, "**Faulty Line Identification Algorithm for Secured Backup Protection Using PMUs**," *Electric Power Components and Systems*, Vol. 45, No. 5, pp. 491-504, 2017.

[30] J. Quanyuan, L. Xingpeng, W. Bo, and W. Haijiao, "**PMU-Based Fault Location Using Voltage Measurements in Large Transmission Networks**," *IEEE Transactions on Power Delivery*, Vol. 27, No. 3, pp. 1644-1652, 2012.

[31] S. Barman and B. K. S. Roy, "**Detection and location of faults in large transmission networks using minimum number of phasor measurement units**," *IET Generation, Transmission & Distribution*, Vol. 12, No. 8, pp. 1941-1950, 2018.

[32] M. K. Neyestanaki and A. M. Ranjbar, "**An Adaptive PMU-Based Wide Area Backup Protection Scheme for Power Transmission Lines**," *IEEE Transactions on Smart Grid*, Vol. 6, No. 3, pp. 1550-1559, 2015.

[33] V. K. Gaur and B. Bhalja, "**New fault detection and localisation technique for double-circuit three-terminal transmission line**," *IET Gener. Transm. Distrib.*, Vol. 12, No. 8, pp. 1687–1696, 2018.

[34] N. Peng, L. Zhou, R. Liang, X. Xue, G. Piliposyan, and Y. Hu, "**Fault location on double–circuit transmission lines by phase correction of fault recorder signals without accurate time synchronization**," *Electric Power Systems Research*, Vol. 181, 2020.

[35] A. Swetapadma and A. Yadav, "**A novel single-ended fault location scheme for parallel transmission lines using k-nearest neighbor algorithm,**" *Comput. Electr. Eng.*, Vol. 69, No. April 2017, pp. 41–53, Jul. 2018.

[36] M. Gil, A. A. Abdoos, and M. Sanaye-Pasand, "**A precise analytical method for fault location in double-circuit transmission lines**," *Int. J. Electr. Power Energy Syst.*, Vol. 126, No. PA, p. 106568, Mar. 2021.

[37] A. Saber, H. H. Zeineldin, T. H. M. El-Fouly, and A. Al-Durra, "**Time-Domain Fault Location Algorithm for Double-Circuit Transmission Lines Connected to Large Scale Wind Farms**," *IEEE Access*, Vol. 9, pp. 11393–11404, 2021.

[38] A. Saber, A. Emam, and H. Elghazaly, "**New fault location scheme for three-terminal untransposed parallel transmission lines,**" *Electr. Power Syst. Res.*, Vol. 154, pp. 266–275, Jan. 2018.

[39] A. Ghorbani , H. Mehrjerdi, "**Accurate fault location algorithm for shunt-compensated double circuit transmission lines using single end data**," *Int J Electr Power Energy System*, Vol 116, 105515, 2020.

[40] M Kundu, S. Debnath. "**Fault location in UPFC compensated double circuit transmission line using negative sequence current phasors**," *Electr Power Syst Res.earch*, Vol. 184, 106347, 2020.

[41] B. K. Saha Roy, A. K. Sinha, and A. K. Pradhan, "**An optimal PMU placement technique for power system observability**," *International Journal of Electrical Power & Energy Systems*, Vol. 42, No. 1, pp. 71-77, 2012.

[42] M. K. Jena, S. R. Samantaray, and B. K. Panigrahi, "**A New Wide-Area Backup Protection Scheme for Series-Compensated Transmission System,**" *IEEE Systems Journal*, Vol. 11, No. 3, pp. 1877-1887, 2017.

[43] B. Naduvathuparambil, M. C. Valenti, and A. Feliachi, "**Communication delays in wide area measurement systems**," in *Proc. 34th Southeast. Symp. Syst*. Theory, Huntsville, AL, USA, Mar. 2002, pp. 118–122.

[44] Mohammad Shahidehpour; Yaoyu Wang, "**Appendix C: IEEE30 Bus System Data**," in *Communication and Control in Electric Power Systems*: Applications of Parallel and Distributed Processing , IEEE, 2003, pp.493-495.

[45] P. Chaiwan, N. Kang, and Y. Liao, "**New accurate fault location algorithm for parallel transmission lines using local measurements**," *Electr. Power Syst. Res*., Vol. 108, pp. 68–73, 2014.

[46] N. I. Elkalashy, T. A. Kawady, W. M. Khater, and A. M. I. Taalab, "**Unsynchronized Fault-Location Technique for Double-Circuit Transmission Systems Independent of Line Parameters**," *IEEE Trans. Power Deliv*., Vol. 31, No. 4, pp. 1591–1600, 2016.

[47] S. Wang and D. Zhao, "**A new false-root identification method based on two-terminal fault location algorithm for double-circuit transmission lines,**" *IEEJ Transactions on Electrical and Electronic Engineering*, Vol. 12, No. 6, pp. 867-873, 2017.

[48] Z.Y. He, R. K. Mai, W. He, Q. Q. QAINS., "**Phasor – measurement-unit based transmission line fault location estimator under dynamic conditions**." *IET Generation, Transmission & Distribution*, Vol. 5, No. 11, pp. 1183-1191, 2011.

[49] T. Hinge and S. Dambhare, "**Synchronised/unsynchrnised measurements based novel fault locatin algorithm for transmission line.**" *IET Generation, Transmission & Distribution*, Vol. 12, No. 7, pp. 1493-1500, 2017.

[50] J. Zare, F. Aminifar and M. Sanaye-Pasand, "**Synchrophasor-Based Wide-Area Backup Protection Scheme with Data Requirement Analysis**," *IEEE Transactions on Power Delivery*, Vol. 30, No. 3, pp. 1410-1419, 2015.